

Laser Guide Star Facility Upgrade

Steffan Lewis¹
 Domenico Bonaccini Calia¹
 Bernard Buzzoni¹
 Philippe Duhoux¹
 Gerhard Fischer¹
 Ivan Guidolin¹
 Andreas Haimerl¹
 Wolfgang Hackenberg¹
 Renate Hinterschuster¹
 Ronald Holzlöhner¹
 Paul Jolley¹
 Thomas Pfrommer¹
 Dan Popovic¹
 Jose-Luis Alvarez¹
 Juan Beltran¹
 Julien Girard¹
 Laurent Pallanca¹
 Miguel Riquelme¹
 Frédéric Gonte¹

¹ ESO

The Laser Guide Star Facility is part of VLT Unit Telescope 4 and provides a single centre-launched sodium beacon for the two adaptive optics instruments SINFONI and NACO. The original facility, installed in 2006, employed a high-power dye laser source, PARSEC, producing an output beam that was delivered via a single-mode optical fibre to launch optics located behind the telescope secondary mirror. We recently installed a new prototype laser source, PARLA, based on Raman optical fibre technology. Requirements for the new laser include start-up times compatible with flexible observing, an output beam appropriate for the existing fibre-delivery system and an on-sky power of up to 7 watts. This is the first time that this type of laser has been deployed at a major observing facility, and it has a pathfinder role for future adaptive optics systems. Reported here are the main results of the development, deployment and early operation since the resumption of science operation in February 2013.

The Laser Guide Star Facility

The main parts of the Laser Guide Star Facility (LGSF) installed on the Very Large Telescope Unit 4 (VLT UT4, Yepun) and described by Bonaccini Calia et al. (2006), are shown in Figure 1. These

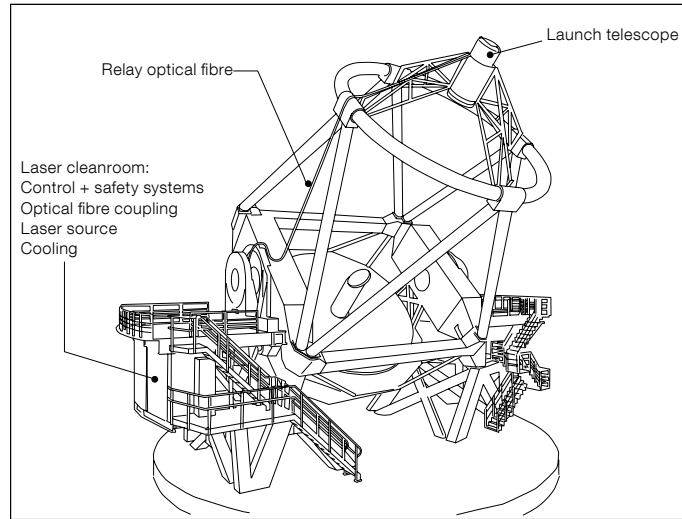


Figure 1. Sketch of VLT UT4 showing the main parts of the Laser Guide Star Facility.

include a laser cleanroom below the Nasmyth platform, an optical fibre beam relay and a launch optical system behind the telescope secondary mirror.

The laser cleanroom contains the bulk of the control and safety electronics, the optical fibre coupling system, and the laser source. In the original facility, the laser source was a dye laser system, PARSEC (Rabien et al., 2003), specified to produce a single-frequency spectral line centred on the sodium D_{2a} line at wavelength of 589.2 nm. The output beam from this laser was transmitted to the input of the relay optical fibre via a free-space beam relay on the laser bench. The role of this beam relay is to format the beam spatially and spectrally, and to actively stabilise the beam position and direction in order to maintain the optical fibre coupling efficiency during operation. Spectral formatting consists of broadening the laser line using a phase modulator in order to increase the total power that can be transmitted through the relay optical fibre.

A large mode area solid-core photonic crystal optical fibre transports the high-power visible laser beam from the laser cleanroom to the launch optics located behind the VLT UT4 secondary mirror. This optical fibre has a length of 27.5 metres, a core mode field diameter of approximately 14 μm and a numerical aperture of 0.04. Transmission losses, excluding input coupling, are approximately 10%.

The launch optics, mounted behind the secondary mirror of the main telescope, receive the visible-light output from the relay fibre and propagate a nearly collimated 50 cm diameter beam onto the sky. They provide beam expansion, focusing, tip-tilt beam stabilisation and diagnostic functionality.

The scope of the upgrade reported here was to install a new prototype laser source. Other subsystems of the LGSF are essentially unchanged.

Sodium excitation

A sodium laser guide star (LGS) is formed by resonantly back-scattering laser light from atomic sodium in the upper mesosphere and lower thermosphere (abbreviated MLT). Optimisation of the laser format to maximise the return flux is being actively studied (Holzlöhner et al., 2010).

Optical radiation at 589 nm was first observed in the night-sky spectrum by V. M. Slipher in 1929 (Slipher, 1929). This radiation was later attributed to emission from neutral sodium atoms occurring mainly in the upper mesosphere (Bernard, 1939), excited by solar radiation. Lying above the range of aircraft, but below the altitude of orbiting spacecraft, the mesosphere is one of the least accessible and most poorly characterised regions of the Earth's atmosphere. Typically it is studied with sounding rockets or observed remotely using laser light detec-

tion and ranging (LIDAR) systems, and from satellites.

The region where atomic sodium is present lies at an altitude range of around 80–120 kilometres with some seasonal variation as well as latitude dependencies. The MLT is one of the coldest regions on Earth, at a temperature of around 180 K. This region is characterised by a number of other features including strong zonal winds, atmospheric tides and overturning gravity waves. Amongst the metals present there are Fe, K, Ca and Na, and it is generally held that this layer of metal atoms and ions is replenished by micro-meteors in the microgram range, that is, interplanetary dust particles that are incident on the Earth and ablated in the upper atmosphere.

Although Fe is the most abundant metal atom in this region, Na is used for LGS applications because it has the highest product of abundance and optical transition cross-section at an accessible laser wavelength. Its mean column density is $4 \times 10^9 \text{ cm}^{-2}$, which is a factor of 10^{-8} of the number for air molecules present in that region. At the lower boundary of the sodium layer, the concentration of oxygen radicals, which originate from ozone, is high enough to form products of sodium hydroxyl and other molecules, and thus remove atomic sodium. Above a temperature-dependent threshold, this process appears to be very efficient and the lower edge of the sodium layer is more sharply defined than the upper edge, where ablated sodium ions recombine with electrons from the ionosphere and from Solar radiation to form atomic sodium.

The sodium *D*-line, which is split into a fine structure doublet D_1 and D_2 at vacuum wavelengths of 589.76 nm and 589.16 nm respectively, contributes to the atmospheric air-glow and is responsible for the familiar orange–yellow light from high-pressure sodium street-lamps. The D_2 -transition is approximately twice as strong as the D_1 , and it is therefore the most efficient target for LGS generation. Despite this, the sodium layer is optically thin and on average only 4% of the incident laser light is actually absorbed, with most of the remainder propagating into outer space. As a further complication, the D_2 line is hyperfine split into a closely

spaced doublet known as D_{2a} and D_{2b} with a ratio of transition strengths of 5:3. These two transitions are separated by about 1.77 GHz, and under mesospheric conditions they partially overlap due to Doppler broadening of each line to a full width half maximum of about 1.07 GHz. There are many additional factors influencing the return flux, such as the laser temporal, spectral and polarimetric format as well as the Earth's geomagnetic field. Calculations of sodium return flux typically make extensive use of computer simulation. Nevertheless, most deployed laser systems to date have concentrated on exciting the D_{2a} -transition, simply because it has the highest peak transmission cross-section.

For the particular case of the LGSF, simulations also suggest that a single narrow line at the peak of the D_{2a} line would be the optimum format to maximise return flux per watt of launched optical power. In practice, the photonic crystal relay fibre is an important factor determining the optical power and launched laser format. This optical fibre does not preserve the polarisation state of the laser beam and stimulated Brillouin scattering, a nonlinear optical effect, limits the maximum power spectral density that it can transmit to approximately 2.7 watts per spectral line, for lines that are sufficiently well separated. Therefore, the single-frequency line produced by the PARLA laser was spectrally broadened using a sinusoidal phase modulator in order to launch a greater number of spectral lines into the existing relay optical fibre and hence more optical power onto the sky. The phase modulation is characterised by the modulation frequency and the amplitude of the peak phase shift measured in radians. The resulting broadened laser spectrum consists of multiple lines forming a frequency comb inside an overall intensity envelope, where the power of each individual line is required to remain below the limit for the relay optical fibre. The comb spacing is equal to the 110 MHz frequency of the phase modulator, and the width of the amplitude envelope and the number of lines in the final laser spectrum increases monotonically with the peak phase shift.

The optimum phase shift for the laser beam is a trade-off between the total power transmitted through the fibre and

the overlap between the broadened multi-line laser spectrum and the sodium D_{2a} atomic transition. The overlap decreases progressively from 100% at zero peak phase shift to 67% at a peak phase shift of 3.76 rad, which is close to the maximum accessible with our equipment. A peak phase shift of around 2.6 rad, corresponding to five spectral lines, was selected for the installed system for a total power of 7 watts exiting the relay fibre. During laboratory tests it was also verified that the spectrum did not change measurably after propagation through the relay fibre and no signal was measured at longer wavelengths where one would expect to find spectral components due to Raman scattering in the glass optical fibre if they were present.

PARLA laser system

The PARLA laser source is based on similar technology to systems that are under development for other ESO projects, which have been described in detail elsewhere (see Bonaccini Calia et al., 2010; Arsenault et al., 2006; and Kaenders et al., 2010). Key elements include a seed laser, a high-power Raman optical fibre amplifier and an efficient frequency doubling scheme. The main optical train is shown in Figure 2. Requirements for the system include flexible observing, high availability, excellent beam quality and stability compatible with the existing optical fibre beam relay.

The laser system includes an electronics cabinet and a laser head which emits a free-space TEM_{00} laser beam with a maximum output power of 20.5 watts at 589 nm. Although this is a 20-watt-class system, the final operating point of the laser source in the installed system is only around 11 watts to achieve the required 7 watts launched power on sky. The laser line-width is specified to be less than 20 MHz, and the centre frequency is tuneable around the centre of the sodium D_2 atomic transition.

Downstream from the laser head, a periscope, phase modulator, and a beam expander unit relay the optical beam to the existing optical fibre coupling system (see Figure 2). The laser includes a stand-alone computer-controlled system that is

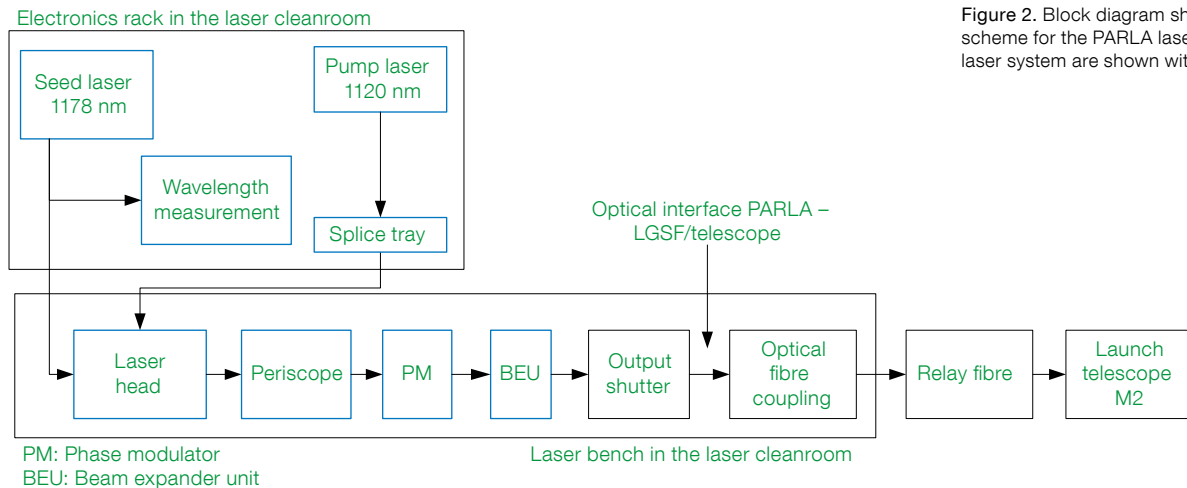


Figure 2. Block diagram showing the main optical scheme for the PARLA laser. The parts of the new laser system are shown with a blue outline.

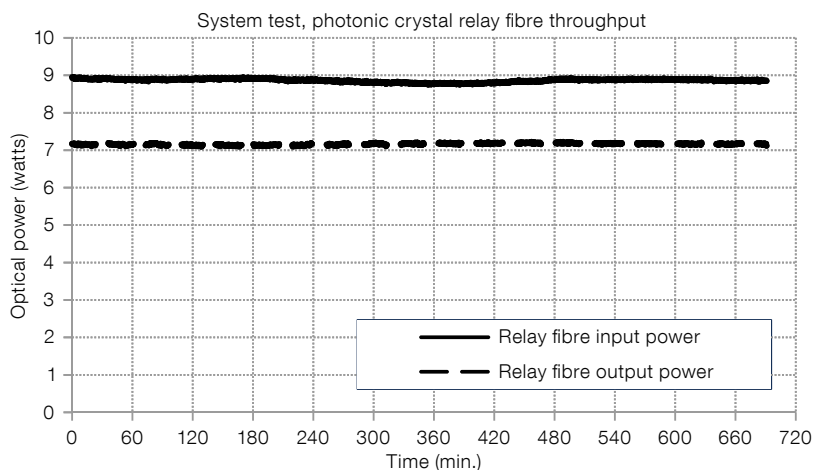


Figure 3. The input and output optical power measured through the relay fibre during the test in the laboratory in Europe is plotted. The average throughput is 80.8%.

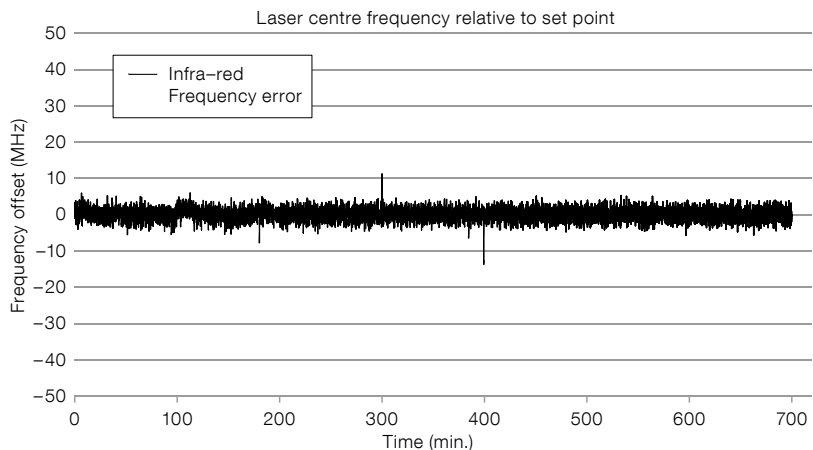


Figure 4. Variation of the laser central frequency measured during the test in Europe is plotted for a period of nearly 12 hours.

connected via a point-to-point Ethernet link to a VLT local control unit (LCU). This interface makes it possible, in a very simple way, to integrate the PARLA laser into the standard VLT control system at the Paranal Observatory.

Results from laboratory system tests, carried out in Europe, are shown in Figures 3 and 4. The laser was tested with a spare relay optical fibre in order to replicate the optical interface to the telescope. The duration of this particular test was 12 hours. Figure 3 shows the optical power at the input and output of the relay fibre. The output power was measured with a bolometer, and the fibre input power was measured using a calibrated pick-off mirror at the fibre input. During this test, the direction and lateral position of the laser beam at the input to the relay optical fibre were actively stabilised using an automated closed loop system, as is the case at the telescope. The average power at the input to the relay fibre was 8.86 watts, the output power 7.16 watts, and the average optical fibre throughput was 80.8%. The throughput includes both the transmission losses of the relay optical fibre (approximately 10%) and the input coupling losses, implying an input coupling efficiency of around 90%.

The infrared laser wavelength was also measured and logged during the test and Figure 4 shows the measured frequency error, in MHz, from the nominal set point during the test. The deviation is within a few MHz, which meets the goal



Figure 5. Image of VLT UT4 (Yepun) during the PARLA commissioning, taken on 14 February 2013.

of 20 MHz. In addition to the selected optical characteristics described above, the laser system was subject to a comprehensive set of performance and functional tests, including the control system and interface to the VLT control software.

Installation and commissioning

The laser was installed on the telescope at the start of 2013, and commissioning took place in February 2013. The commissioning process included standalone tests of the LGSF with the new laser subsystem, and commissioning and science verification (SV) with the complete observing system and the two adaptive optics instruments, SINFONI and NACO. Figure 5 shows a photograph of UT4 taken during the commissioning in February 2013.

The LGS was first commissioned in a standalone mode, before the start of observations and SV tests with the instruments. To verify the correct output wavelength, the centre frequency of the laser system was scanned in steps of 250 MHz and 100 MHz around the nominal centre of the sodium D_{2a} transition and the relative return flux (brightness) of the LGS was measured using the UT4 guider camera. The guider output is in analogue-to-digital units (ADU) which are nominally linear with the flux. Figure 6 shows the plot of return flux versus laser wavelength taken during on-sky calibration. The measured line shape is a convolution of the laser spectrum and the Doppler-broadened sodium D_2 transition; the doublet is therefore not fully resolved. The main peak corresponds to the D_{2a} transition and the broad shoulder in the high frequency side corresponds to the sodium D_{2b} transition. The laser was tuned to the peak of the D_{2a} line, determined on sky in the final configuration.

The angular size subtended by the LGS was measured using the telescope guide camera at different altitudes and is listed in Table 1. Images of a natural guide star were taken before each LGS measurement and used to infer the seeing. The exposure time for the LGS images was approximately 2 seconds. This exposure duration averages the majority of the seeing effect, but formally

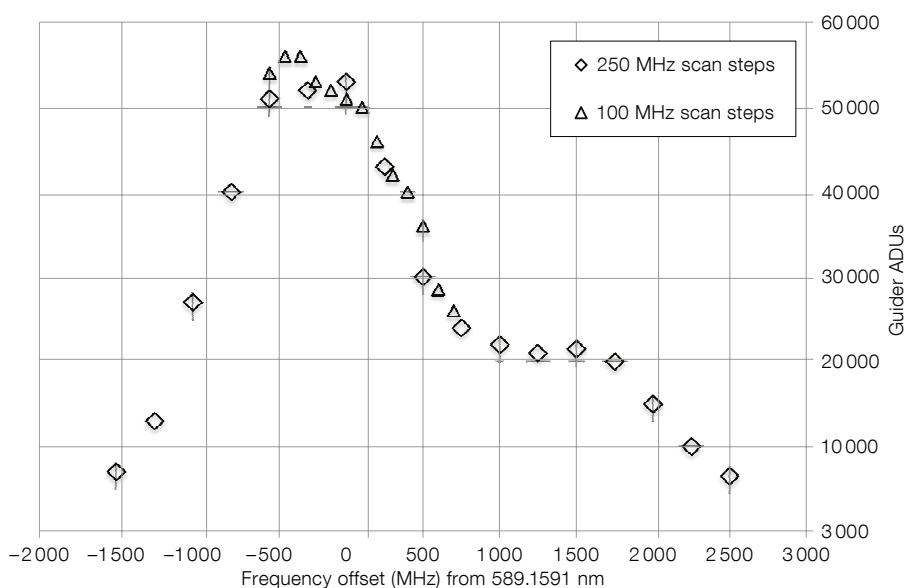


Figure 6. A wavelength scan through the sodium D_2 doublet taken during commissioning.

speaking is too short to qualify as a true long-exposure measurement of the spot size.

The return flux, and apparent magnitude, of the LGS were not measured photometrically. However, the counts from the SINFONI wavefront sensor, which is based on photon-counting avalanche photodiodes, were accessible. The wavefront sensor counts and the system performance during SV were the two metrics used to verify that the return flux was sufficient to meet the operational requirements. Measurements of the apparent LGS magnitude were made using SINFONI at different altitudes and at different times during the commissioning period. Typically the flux measured on the wavefront sensor equated to around 6 million counts per second. The optical power launched onto the sky was between 6 and 7 watts during these tests. This level of photon return was found to be sufficient to achieve good closed-loop adaptive optics performance during SV.

At the time of commissioning further measurements needed to be done before a definitive comparison could be made between the measured and theoretical return flux for this system. The principal uncertainty is the sodium abundance, which has been shown to vary by a factor of four seasonally (Simonich et al., 1979) and by a factor of up to two during a single night. Frequent measurements taken at different times of the year are therefore necessary.

Table 1. Measurements of the natural guide star (NGS) and laser guide star angular size.

Zenith angle (deg)	NGS size (arcsec)	LGS size (arcsec)
19.4	0.55	1.16
19.4	0.68	1.28
24.6	0.66	1.34
36.2	0.92	1.59
41.7	0.88	1.79
54.9	0.90	1.62

Science verification

The observing targets selected for SV are given in Table 2. These were repeats of existing and already published observations.

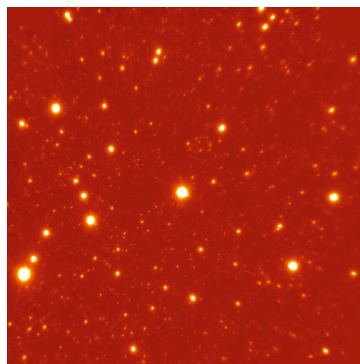


Figure 7. K_s -band NACO image of part of the globular cluster Omega Centauri. The field of view is 37 arcseconds square and the seeing was 0.75 arcseconds. The full width half maximum of star images is between 0.094 and 0.11 arcseconds.

Instrument	Object name	Description
NACO	NGC 3621	Bulgeless galaxy
NACO	Centaurus A	Active galactic nucleus
NACO	NGC 5139	Globular cluster, Omega Centauri
SINFONI	Haumea (TNO136108)	Trans-Neptunian object
SINFONI	NGC 36210.90	Bulgeless galaxy

Table 2. Science verification targets.

The observations selected for NACO were successfully executed during the commissioning nights. Observations were mainly made with the 7×7 wavefront sensor, and the adaptive optics loop remained closed without problems down to an altitude of 30 degrees during standard operation tests. The instrument was operated in a number of different configurations: tip-tilt correction only, high-order correction only, and with full correction. On the night of 17 February 2013 with full correction, Strehl ratios in the range 15.6–37% in the K_s -band were measured in seeing ranging from 0.76 to 0.99 arcseconds, as recorded by the differential image motion monitor (DIMM) at 500 nm. Figure 7 shows an image of the cluster in Omega Centauri taken on another commissioning night. The field of view is 37 by 37 arcseconds, the seeing was 0.75 arcseconds and the coherence time $\tau_0 = 3.7$ ms. The full width half maximum of the stars is between 0.094 and 0.11 arcseconds with full adaptive optics correction.

The observations of Haumea and NGC 3621 with SINFONI were also completed successfully. SINFONI was able to work stably in closed loop with the laser during standard operation tests. When observing the trans-Neptunian object Haumea, it was possible to observe up to the twilight limit without problem. For the last two nights of the planned commissioning period the sys-

tem was handed back to science operations for service observing.

Operation

At the time of writing, the LGSF has been operating with the PARLA laser for almost one year.

One of the goals of the laser upgrade was to enable flexible observing. By this it is meant that the laser can be available for science observation within a short period of time, formally specified as 30 minutes, should the need or opportunity arise for a laser-supported observation. To achieve this aim, an idle state was defined in which the laser waits in a low-power configuration. In this scheme, the lifetime of the high-power optical components is extended by reducing their usage outside of actual observing time, while still ensuring that the system is available at short notice. This is a significant change from the original laser system which ran continuously at high power when it was available. In the new implementation, the telescope operator can wake up the laser using an automated script from the control room and be ready for operation in approximately ten minutes. Figure 8 shows the availability of the LGSF in hours per month for the first six months of operation after the upgrade.

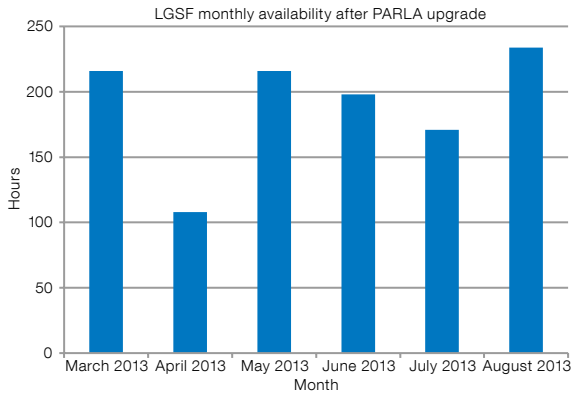


Figure 8. Availability of the LGSF for the first six months of science operation after the upgrade is plotted, in hours per month.

After some months of operations with PARLA, the scientific use of the LGSF has increased very significantly to about 35 hours per month on average (SINFONI only). Remaining non-availability (see Figure 8) has a < 15% impact on the total LGSF scientific use. The reliability of PARLA has made it possible to tackle other control issues, especially for SINFONI Multi-Applications Curvature Adaptive Optics (MACAO). Observations with the LGSF are now performed with significantly fewer overheads and in a more reliable way, providing that the atmospheric conditions are suitable.

The photon return flux, defined as the number of photons per unit area per second returning from the LGS, is also of interest over long timescales due to the large seasonal variability of this parameter (Holzlöhner et al., 2010; Simonich et al., 1979). Automated logging of the num-

ber of counts on the SINFONI wavefront sensor can be used as a relative measure, although instrumental effects preclude a photometric analysis. Figure 9 shows the mean and standard deviations of the wavefront sensor counts in a monthly time series. These values include contributions from the complete observing system and there is not necessarily a direct correspondence with the atmospheric sodium column abundance.

Prospects

The LGSF at the Paranal Observatory has been upgraded with a prototype laser source based on Raman fibre laser technology. This is the first time that this type of laser has been operated as part of a major astronomical observing facility. Results from almost one year of science operation have shown that the LGSF can be used more flexibly and with significantly higher availability after the upgrade. Experience with this system is providing valuable feedback for the ESO Adaptive Optics Facility, currently under develop-

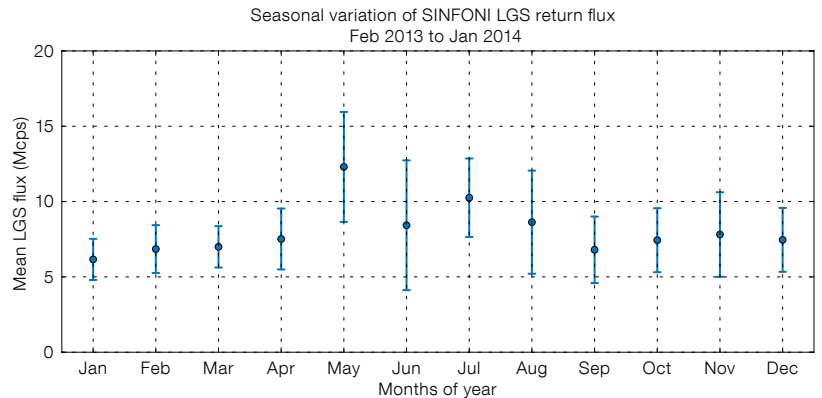


Figure 9. Monthly means and standard deviations of the counts, recorded by the SINFONI wavefront sensor, for the laser guide stars over the period of the upgraded LGSF.

ment, which will deploy four complete LGS units on the centrepiece of VLT UT4.

Acknowledgements

We would like to acknowledge the support of Roberto Tamai for this project. We would also like to thank Nadine Neumayer and Yazan Al Momany for processing and reducing the science images and Jared O'Neal for work on system performance monitoring. We would like to thank the following companies for their support: Topica Photonics AG, MPB Communications Inc. and Mitsubishi Cable.

References

- Arsenault, R. et al. 2006, *The Messenger*, 123, 6
- Bernard, R. 1939, *ApJ*, 89, 133
- Bonaccini Calia, D. et al. 2006, *SPIE*, 6272, 627207
- Bonaccini Calia, D. et al. 2010, *SPIE*, 7736, 77361U-1
- Holzlohner, R. et al. 2010, *A&A*, 510, A20
- Kaenders, W. G. et al. 2010, *SPIE*, 7736, 773621
- Rabien, S. et al. 2003, *SPIE*, 4839, 393
- Simonich, D., Clemesha, B. & Kirchhoff, V. 1979, *J. Geophys. Res.: Space Phys.*, 84, 1543
- Slipher, V. M. 1929, *PASP*, 41, 262



A colour image of the polar ring galaxy NGC 4650A is shown. The image was formed by colour-coding the MUSE spectral cube (range 4800–9300 Å) obtained during the instrument commissioning run in February 2014. See Release eso1407 for more details.